Single-Dirac-Cone Topological Surface States in the $TlBiSe_2$ Class of Topological Semiconductors

Hsin Lin,[1] R. S. Markiewicz,[1] L. A. Wray,[2,3] L. Fu,[4] M. Z. Hasan,[2,3] and A. Bansil[1]

[1]*Department of Physics, Northeastern University, Boston, Massachusetts 02115, USA*
[2]*Joseph Henry Laboratories of Physics, Princeton University, Princeton, New Jersey 08544, USA*
[3]*Princeton Center for Complex Materials, Princeton University, Princeton, New Jersey 08544, USA*
[4]*Department of Physics, Harvard University, Cambridge, Massachusetts 02138, USA*

(Received 18 March 2010; published 16 July 2010)

We investigate several strong spin-orbit coupling ternary chalcogenides related to the (Pb,Sn)Te series of compounds. Our first-principles calculations predict the low-temperature rhombohedral ordered phase in $TlBiTe_2$, $TlBiSe_2$, and $TlSbX_2$ (X = Te, Se, S) to be topologically nontrivial. We identify the specific surface termination that realizes the single Dirac cone through first-principles surface state computations. This termination minimizes effects of dangling bonds, making it favorable for photoemission experiments. In addition, our analysis predicts that thin films of these materials could harbor novel 2D quantum spin Hall states, and support odd-parity topological superconductivity.

DOI: 10.1103/PhysRevLett.105.036404 PACS numbers: 71.20.Nr, 71.10.Pm, 73.20.At

Topological insulators are a recently discovered new phase of quantum matter [1–3]. The search for topological insulators in real materials has benefited from the fruitful interplay between topological band theory and realistic band structure calculations [4–12]. As a result, Bi_xSb_{1-x}, Bi_2Se_3, and Bi_2Te_3 have been experimentally realized as three-dimensional topological insulators [6–8,10–12]. Recently, this search has been extended to ternary compounds [13,14]. Here, we report first-principles band calculations of the Tl-based III-V-VI_2 ternary chalcogenide series, and compare the results to those of the related (Pb, Sn)Te series studied previously in connection with Dirac fermion physics in the 1980s [15]. The low-temperature rhombohedral ordered phase in $TlBiTe_2$, $TlBiSe_2$, and $TlSbX_2$ (X = Te, Se, S) is predicted to be topologically nontrivial. Moreover, we have carried out first-principles slab computations in order to identify the specific surface termination which gives rise to the simple Dirac-cone surface band. An analysis of the symmetry of states indicates that thin films of the present materials would support 2D-quantum spin Hall states.

Designing new topological insulators involves modifying atomic structure or doping to shift band orders out of the natural sequence. Consider, for example, the well-known case of (Pb,Sn)Te with a rocksalt structure. The end phase PbTe with a face-centered cubic (fcc) lattice is topologically trivial. In contrast, SnTe has band inversions at four equivalent L points where parities of conduction and valence bands are switched [Fig. 2(e)]. Since this inversion occurs at an even number of points in the Brillouin zone, SnTe is also a topologically trivial band insulator. Fu and Kane [5] proposed that a rhombohedral distortion along a particular 111 direction can induce (Pb, Sn)Te into a strong topological phase because then the band inversion occurs only at the L point along the 111 direction which is distinguished from the other three L points [Fig. 1(b)].

The Tl-based III-V-VI_2 ternary chalcogenides $MM'X_2$ are, or can be, approximately viewed as a rhombohedral structure with space group $R\bar{3}m$ [16] with a center of inversion symmetry. The unit cell contains four atoms: M = Tl, M' = Bi or Sb, and X = Te, Se, or S atoms, which occupy the Wyckoff 3a, 3b, and 6c positions, respectively. If $M = M'$ and the corresponding hexagonal lattice constants a and c satisfy the relation $c = 2\sqrt{6}a$, a rocksalt fcc structure is restored with $a' = \sqrt{2}a$ with only two atoms/unit cell. The rhombohedral lattice is embedded in a $2 \times 2 \times 2$ supercell of the fcc lattice as shown in Fig. 1(a). This relation between rhombohedral and fcc lattices is analogous to the type-II antiferromagnet NiO with M = Ni spin up, M' = Ni spin down, and X = O. In this sense, Tl-based III-V-VI_2 ternary chalcogenides constitute an offshoot of the IV-VI semiconductors and can be called pseudo IV-VI semiconductors [17–22]. Taking the example of $TlBiTe_2$, because Tl and Bi precede and follow Pb in the periodic table, $TlBiTe_2$ resembles PbTe where

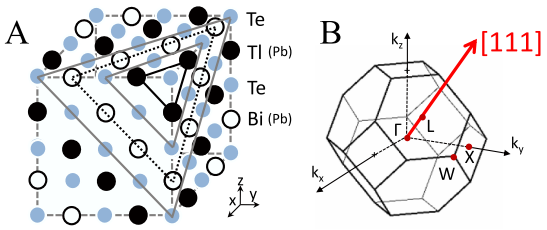

FIG. 1 (color online). (A) Crystal structure of idealized fcc $TlBiTe_2$. The Tl surface is emphasized by black lines, the Bi surface by dotted lines, and the Te surface by gray lines. (B) The fcc Brillouin zone. The thick red arrow marks the 111 rhombohedral distortion direction.

$M = M' =$ Pb. Therefore, by distorting the PbTe crystal along a 111 direction and replacing Pb by Bi and Tl alternating along that 111 direction, one obtains $TlBiTe_2$ with a rhombohedral structure. In the ordered crystalline phase, the X atom moves away from the fcc position.

Since Tl-based III-V-VI_2 ternary chalcogenides provide a rhombohedral version of (Pb,Sn)Te, one may expect these compounds to display topologically nontrivial phases. We have explored this possibility by performing first-principles calculations [23] within the framework of the density functional theory using the generalized gradient approximation [24]. Spin-orbit coupling was included as a second variational step. The lattice constants were taken from the optimized values given in Table I of Ref. [16].

To better explain the relationship between (Pb,Sn)Te and the Tl-based III-V-VI_2 ternary chalcogenides, Fig. 2 shows the evolution of bands for a sequence of structures going from fcc PbTe [Fig. 2(a)] to $TlSbTe_2$ [Fig. 2(d)]. For fcc PbTe, the top of the valence bands is located at the L points with a small gap. When the same calculation is repeated by assuming a rhombohedral unit cell with two chemical formula units, doubled along a 111 axis, we obtain the folded bands of Fig. 2(b). In particular, the top of the valence band at one L point is folded to the Γ point, and the other three L points are folded to three equivalent X points. Since no distortions are introduced yet, the bands do not interact with the folded bands. In the next step [Fig. 2(c)], we replace one of the Pb atoms by an Sn atom, resulting in alternating Pb and Sn planes along the selected 111 direction. The original and folded bands now interact, inducing new band gaps and avoided crossings for the hypothetical ternary compound $PbSnTe_2$. Otherwise, the band structure is superficially similar to that in Fig. 2(b). The conduction and valence bands now become inverted at high-symmetry points. The band inversion effect can be monitored through the probability of s-orbital occupation (red dots) [25] on the M atom (here $M =$ Pb) at the inversion center. Comparing the band sequence with red dots for PbTe and $PbSnTe_2$, we see that band inversion indeed occurs at both Γ and X points [Fig. 2(f)]. Because of an even number of band inversions, $PbSnTe_2$ is also topologically trivial similar to SnTe. But, since $PbSnTe_2$ only has rhombohedral instead of cubic symmetry, its band gaps at the Γ and X points become unequal. The band gaps at X points are smaller, which indicates that band inversion from PbTe to $PbSnTe_2$ occurs first at Γ and then at X. This suggests that by introducing a small rhombohedral lattice distortion or by replacing Pb and Sn with other atoms, the second band inversion associated with the three X points might be removed, leaving only a single band inversion relative to PbTe (in a supercell) at Γ, which would lead to a topologically nontrivial band structure. This leads us to replace Pb (Sn) by Tl (Sb) and introduce rhombohedral lattice distortion to obtain the bands in Fig. 2(d), which resemble those of (Pb,Sn)Te. The rhombohedral lattice distortion enhances all band gaps, especially at Γ, and shifts the band edges at the X points. The bottom of the conduction band at the X point overlaps the top of the valence band at a low-symmetry point (not shown), leading to a semimetal ground state. Nevertheless, since a direct band gap between the conduction and valence bands exists throughout the Brillouin zone, the Z_2 topology of the valence bands is well defined. To determine the band topology, one should focus on the band inversion relative to supercell PbTe at Γ and three X points. The s-orbital occupation in Fig. 2(d) shows that band inversion occurs at all four points as in $PbSnTe_2$. Hence, with fcc atomic positions, $TlSbTe_2$, and indeed all six Tl-based III-V-VI2 ternary chalcogenides presented here, would be topologically trivial semimetals.

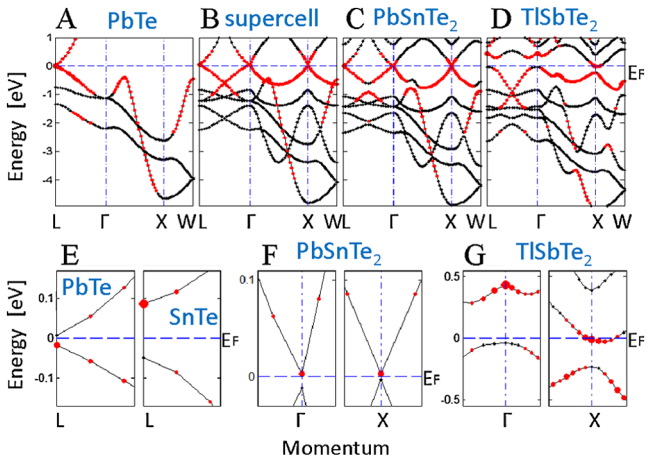

FIG. 2 (color online). (A)–(D) Band structures of PbTe, PbTe in a supercell rhombohedral structure with 4 atoms/unit cell, $PbSnTe_2$, and $TlSbTe_2$ with fcc atomic positions. The fcc symbols for points in the Brillouin zone are used as in Fig. 1(b) for ease of comparison. The size of the red dots denotes the probability of s-orbital occupation on the M atoms. (E) Band inversion at L for SnTe relative to PbTe. Panels (F) and (G) highlight band inversion at the Γ and X points for $PbSnTe_2$ (C) and $TlSbTe_2$ (D), respectively.

However, experiments [18,21,22] find that the X atom moves away from the fcc position towards the M' layer in the ordered crystalline phase. We define z_X to be the distance away from the fcc position for the X atom. Figure 3 gives band structures of $TlSbTe_2$ for the density-functional-theory–generalized-gradient-approximation total-energy optimized $z_{Te} =$ 0.21 Å value as well as for two shifted values of z_{Te} to illustrate the sensitivity of band structure to the value of z_{Te}. The optimized value is in good agreement with experiments [22]. For $z_{Te} = 0$, the band parities at Γ and M have the same ordering as that in SnTe [Fig. 2(e)] or $PbSnTe_2$ [Fig. 2(f)], and the material is topologically trivial. For $z_{Te} = 0.21$ Å, the band parity at the X point changes and the Z_2 index picks up a factor of -1. In addition, the gap between the conduction and valence bands becomes large enough to make the compound an insulator. Thus, $TlSbTe_2$ is predicted to be a topological insulator for the optimized

Te position. For $z_{\mathrm{Te}} = 0.33$ Å, the gap at Γ is close to zero. As Te atoms move further away, the material once again becomes topologically trivial with $Z_2 = 1$. The range of z_{Te} values which yield a nontrivial phase is shown by the gray area in Fig. 3(e). This range can be ascertained by monitoring the gap sizes at Γ and X. At the critical point where the band inverts, the gap goes to zero. We have repeated the preceding procedure for other Tl compounds and found that all these compounds become topologically nontrivial at the optimal X-atom position, except for $TlBiS_2$, which is predicted to be a topologically trivial band insulator [26,27].

In order to test the robustness of our results to effects of band-gap corrections or alloying, we have considered effects of adding an orbital-dependent potential into the Hamiltonian. For Tl-based III-V-VI_2 ternary chalcogenides, the orbital character of the conduction (valence) band is p type for M' (X) atoms. We specifically add orbital-dependent potentials V_a to all three p orbitals of M', which moves the conduction band upwards. As an example, we start with a topologically trivial phase in $TlSbTe_2$ with $z_{\mathrm{Te}} = 0$. With increasing V_a, as Fig. 3(d) shows, the gap at X vanishes at $V_a = 1$ eV and band inversion occurs. This transition occurs for the Γ point at a larger V_a value of 1.6 eV. Between these two critical points, bands are inverted only at the Γ point relative to PbTe and the system becomes topologically nontrivial [shaded area in Fig. 3(d)]. We have found a similar behavior in other compounds of this family. Despite uncertainties inherent in first-principles computations, our calculations

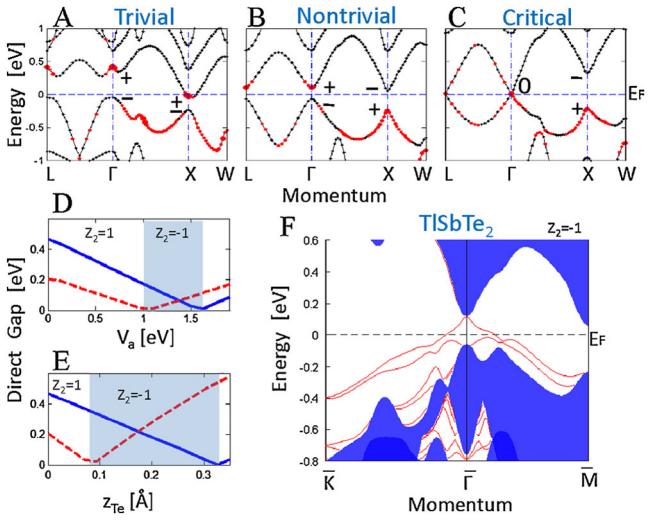

FIG. 3 (color online). Panels (A)–(C) show the bulk band structure of $TlSbTe_2$ for $z_{\mathrm{Te}} = 0$, 0.21, and 0.33 Å, respectively. The fcc notation for the high-symmetry points is used as in Fig. 1(b). Panels (D) and (E) show the direct gaps at Γ (blue solid line) and X (red dashed line) as a function of V_a and z_{Te}, respectively. The gray area highlights features related to topological nontriviality. Panel (F) shows the surface state dispersions at an optimized value of z_{Te} [red (gray) lines]. Projected bulk bands are shown as blue areas.

establish band inversion at Γ and X points (relative to PbTe) as the decisive factor of their topological class.

A nontrivial band topology will generate metallic surface states which are the hallmark of topological insulators. For the 111 surface in Tl-based III-V-VI_2 ternary chalcogenides, the atoms are sequenced as -M-X-M'-X- and there are four possible surface terminations [see Fig. 1(a)]. Unlike Bi_2Se_3 and Bi_2Te_3, the bonding between the layers in $TlM'X_2$ is not weak. As a result, the topologically protected surface states may coexist with nontopological ones arising from dangling bonds, leading to a complicated surface spectrum. We have carried out extensive slab calculations on all possible surface terminations for all six compounds to search for a simple surface spectrum. We find that the number of trivial dangling-bond surface states is minimized for a termination with X atoms exposed and M' atoms beneath the surface, since fewer bonds are broken in forming this surface, making this the likely candidate for the naturally occurring surface. Figure 3(f) shows the surface band structure of $TlSbTe_2$ with optimized atomic positions in a topologically nontrivial phase. The calculation is based on a slab with 47 atomic layers. The Dirac point is at the edge of the conduction band at $\bar{\Gamma}$. Between $\bar{\Gamma}$ and $\bar{M}$, there is only one surface band [red (gray) lines] connecting conduction and valence bands. This is unambiguous evidence for a nontrivial topology.

Even if the compounds are in a topologically trivial phase, their surface states may have Dirac-cone dispersions due to band inversion. In Fig. 4, we show the calculated surface dispersions with $z_{\mathrm{Te}} = 0$ without band-gap corrections for a 23 layer slab, where the X atoms are exposed at both sides of the slab. The slab thickness is about 50 Å. Dirac cones with small gaps are obtained at $\bar{\Gamma}$ and $\bar{M}$ due to the projection of Γ and X points to the surface Brillouin zone. The Dirac cones have smaller gaps at $\bar{\Gamma}$ in $TlSbTe_2$ (A), $TlSbSe_2$ (B), $TlSbS_2$ (C), $TlBiTe_2$ (D), and $TlBiSe_2$ (E), and at $\bar{X}$ in $TlBiS_2$ (F). Consider $TlBiTe_2$ as an example. The gap at Γ decreases rapidly as the slab thickness increases, indicating that a gapless Dirac band exists at Γ on the surface in the infinite thickness limit. Note, however, that the existence of a surface Dirac band at Γ by itself does not reveal the band topology, and the surface spectrum near the $\bar{M}$ points must also be considered. Hence a $k \cdot p$ model around Γ is not adequate for these compounds. In our slab calculations, surface states near $\bar{M}$ have strong finite size effects arising from interactions between the two end surfaces of the slab. This sensitivity to finite size effects could be utilized to design thin film samples which have quantum spin Hall states. In these films, the Dirac points are all gapped, as in Fig. 4, and we can calculate the 2D topological index Z_2 by analyzing only the points $\bar{\Gamma}$ and $\bar{M}$. From wave function parity analysis at these points, illustrated in Fig. 4, we obtain $Z_2 = -1$ for $TlSbTe_2$, $TlSbSe_2$, $TlSbS_2$. Hence these compounds are topologically nontrivial quantum spin Hall systems. In the case of $TlBiTe_2$, the upper and lower Dirac cones are almost degenerate at $\bar{\Gamma}$.

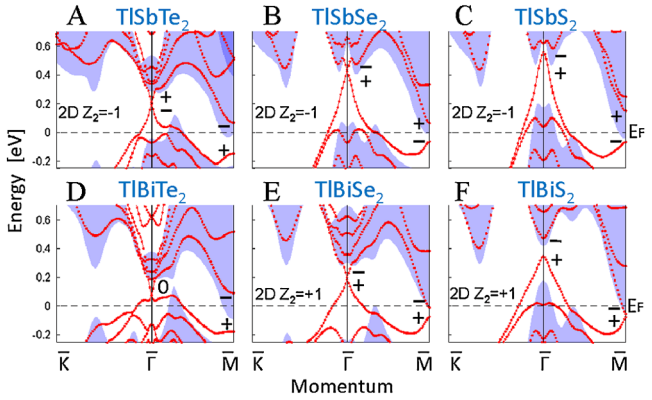

FIG. 4 (color online). Band structures based on thin slab calculations for $TlSbTe_2$ (A), $TlSbSe_2$ (B), $TlSbS_2$ (C), $TlBiTe_2$ (D), $TlBiSe_2$ (E), and $TlBiS_2$ (F) with $z_X = 0$, but without band-gap corrections. The blue (gray) area marks projected bulk bands. Red dots are 2D bands for the thin slab. Parity analysis of states at $\bar{\Gamma}$ and $\bar{M}$ indicates that thin films in panels (A)–(C) would harbor topologically nontrivial 2D quantum spin Hall states.

Interestingly, $AgBiTe_2$, $AgBiSe_2$, and $AgInSe_2$ all possess a crystal structure similar to the present compounds, but with M = Ag. However, our first-principles bulk and surface state computations on these Ag compounds indicate a lack of band inversions. In particular, the surface and bulk bands display similar dispersions, and there is no evidence for the presence of a protected Dirac-cone surface band or other signatures of topologically interesting behavior.

Apart from the fact that Tl compounds are usually semimetallic or very weakly semiconducting, they are topologically similar to the Bi_2Se_3 series discovered previously. Recently, it was found that upon Cu doping, Bi_2Se_3 becomes a superconductor with a $T_c = 3.8$ K and exhibits unconventional band topology [28–30]. The doped topological states in the Tl-based compounds thus are also a likely candidate for finding odd-parity topological superconductors similar to the $Cu_xBi_2Se_3$ series [28–30].

In conclusion, we have shown that the Tl-based III-V-VI_2 ternary chalcogenides are highly favorable for supporting $Z_2 = -1$ topological states. Their topological nature is driven by the band inversions at *both* Γ and X points. We identify the optimal surface termination for single-Dirac-cone surface states and predict that thin films could harbor 2D topologically nontrivial quantum spin Hall states. Our study thus indicates that the present Tl-based compounds constitute a fertile ground for observing and engineering topologically interesting phases of quantum matter.

We acknowledge discussions with R. J. Cava and B. Barbiellini. The work at Northeastern and Princeton is supported by the Basic Energy Sciences, U.S. Department of Energy (DE-FG02-07ER46352, DE-FG-02-05ER46200, and AC03-76SF00098), and benefited from the allocation of supercomputer time at NERSC and Northeastern University's Advanced Scientific Computation Center (ASCC). Support from the A. P. Sloan Foundation (L. A. W. and M. Z. H.) and Harvard University (L. F.) is acknowledged.

[1] M. Z. Hasan and C. L. Kane, arXiv:1002.3895.
[2] J. E. Moore, Nature (London) **464**, 194 (2010).
[3] X.-L. Qi and S.-C. Zhang, Phys. Today **63**, 33 (2010).
[4] B. A. Bernevig *et al.*, Science **314**, 1757 (2006).
[5] L. Fu and C. L. Kane, Phys. Rev. B **76**, 045302 (2007).
[6] D. Hsieh *et al.*, Nature (London) **452**, 970 (2008).
[7] D. Hsieh *et al.*, Science **323**, 919 (2009).
[8] Y. Xia *et al.*, Nature Phys. **5**, 398 (2009).
[9] D. Hsieh *et al.*, Nature (London) **460**, 1101 (2009).
[10] Y. L. Chen *et al.*, Science **325**, 178 (2009).
[11] H. Zhang *et al.*, Nature Phys. **5**, 438 (2009).
[12] D. Hsieh *et al.*, Phys. Rev. Lett. **103**, 146401 (2009).
[13] H. Lin *et al.*, Nature Mater. **9**, 546 (2010).
[14] S. Chadov *et al.*, Nature Mater. **9**, 541 (2010).
[15] E. Fradkin, E. Dagotta, and D. Boyanovsky, Phys. Rev. Lett. **57**, 2967 (1986).
[16] K. Hoang and S. D. Mahanti, Phys. Rev. B **77**, 205107 (2008).
[17] K. M. Paraskevopoulos, J. Phys. C **18**, 4941 (1985).
[18] O. Valassiades *et al.*, Phys. Status Solidi (a) **65**, 215 (1981).
[19] D. V. Gitsu *et al.*, J. Phys. Condens. Matter **2**, 1129 (1990).
[20] K. M. Paraskevopoulos *et al.*, J. Alloys Compd. **467**, 65 (2009).
[21] M. Ozer *et al.*, Semicond. Sci. Technol. **11**, 1405 (1996).
[22] E. F. Hockings and J. C. White, Acta Crystallogr. **14**, 328 (1961).
[23] P. Blaha *et al.*, *WIEN2k* (University of Technology, Vienna, 2001).
[24] J. P. Perdew, K. Burke, and M. Ernzerhof, Phys. Rev. Lett. **77**, 3865 (1996).
[25] Since the probability of s-orbital occupation (denoted by the size of the red dots) must vanish for an odd-parity band at high-symmetry points, we can use this as a measure of band parity.
[26] After completing this work, we became aware of a preprint by Yan *et al.* (Ref. [27]) who predict several of the present Tl compounds to be topological insulators using bulk band computations, extended via the $k \cdot p$ scheme for surface states. While our conclusion concerning the topological nature of these compounds is similar to that of Ref. [27], our analysis based on first-principles bulk and slab computations also identifies the specific surface that features the protected single Dirac cone suitable for photoemission studies. Moreover, we have clarified the relationship of the Tl compounds to PbTe, obtaining insight into pathways for engineering topologically interesting properties more generally.
[27] B. Yan *et al.*, arXiv:1003.0074.
[28] Y. S. Hor *et al.*, Phys. Rev. Lett. **104**, 057001 (2010).
[29] L. A. Wray *et al.*, arXiv:0912.3341v1.
[30] L. Fu and E. Berg, arXiv:0912.3294v1.